Indian Journal of Science and Technology, Vol 9(35), DOI: 10.17485/ijst/2016/v9i35/96501, September 2016
ISSN (Print) : 0974-6846
ISSN (Online) : 0974-5645

sEMG based Classification of Hand Gestures using Artificial Neural Network

G. Emayavaramban* and A. Amudha

Faculty of Engineering, Karpagam University, Coimbatore - 641021, Tamil Nadu, India; emayam1989@gmail.com, amudhac11@yahoo.co.in

Abstract

Objectives: Study of sEMG signals of the hand gestures is important in designing hand prosthesis. Designing a sEMG pattern recognition system to control a myoelectric hand using neural networks is the objective of this study. **Methods/ Statictical Analysis:** The sEMG signal was acquired from flexor digitorumsuperficialis and extensor digitorum muscle of the ten healthy subjects by performing 12 different hand gestures. Six parametric feature extraction algorithms were applied to derive the prominent information from sEMG such as AR (Autoregressive) Burg, AR Yule Walker, AR Covariance, AR Modified Covariance, Levinson Durbin Recursion and Linear Prediction Coefficient. Recognition of the 12 gestures is accomplished using General Regression Neural Network, Probabilistic Neural Network and Radial Basis Function Neural Network. **Findings:** From the empirical results it was observed that the AR Burg and RBFNN combination had the highest recognition accuracy rate of 94.04%. Investigation also proved that recognition accuracy of sEMG signals were better for females when compare to males. It was also observed from the results that subjects in the age of 26-30 years had better muscle flexion compared to the other age groups studied. **Application/ Improvements:** In this paper the feasibility of recognizing twelve hand gestures from the sEMG of the hand and finger movements using neural networks was investigated. Six feature extraction algorithms and three neural networks were used to design algorithms for recognizing the twelve hand gestures

Keywords: Surface Electromyography, Autoregressive, AR Burg, AR Yule Walker, AR Covariance, AR Modified Covariance, Levinson Durbin Recursion, Linear Prediction Coefficient, Radial Basis Function Neural Network, Probabilistic Neural Network, General Regression Neural Network

1. Introduction

Prosthetic arm is an artificial device that restores lost body part. Upper limb amputation may occur through trauma, illness or inborn defect[1-3]. Human Machine Interface (HMI) is widely used to communicate and control the interactions between human and machine. HMI detects the specific pattern activity and translates the pattern into meaningful control commands. Human beings make various hand movements with several tasks such as hand open, hand close which can be used to develop HMI system. This system helps to improve quality level of the amputees. Human–Machine Interfaces have received more attention during the past decade[4,5].

sEMG is an investigation of electrical activity on skeletal muscles which is recorded at the surface of the skin. sEMG is broadly applied for rehabilitation, prosthetic arm control, medical detection and analysis of muscles tiredness. sEMG is standard technique of analysis in HMI and it can be operated by trained person or physician with minimum danger to the participants. One of the advantages of sEMG is non invasive[6-9].

In this study, twelve different hand gestures are performed by the subjects for developing a prosthetic arm. The proposed hand gestures are opening hand, closing hand, thumb extension, thumb flexion, index extension, index flexion, middle extension, middle flexion, ring extension, ring flexion, little extension and little flexion. Six feature extraction algorithms based on AR Burg,

*Author for correspondence

AR Yule Walker, AR Covariance, AR Modified Covariance, Levinson Durbin Recursion and Linear Prediction Coefficient has been applied to excerpt the features from sEMG signals. The extracted features are classified using General Regression Neural Network, Probabilistic Neural Network and Radial Basis Function Neural Network.

2. Research Background

The sEMG signal is an electrical activity, initiated from muscle fibers which are produced by mutual transfer of ions from the muscle fiber membranes. A general model of sEMG signal is given in equation 1

$$x(n) = \sum_{r=0}^{N-1} h(r)\, e(n-r) + w(n) \quad (1)$$

Where w(n) represents white Gaussian noise, x(n) represents general model of sEMG signal, h(r) indicates the MUAP (Motor Unit Action Potential), e(n) shows the firing impulse and n is number of motor unit firings[10].

In[11]the author proposed single channel sEMG for able and amputee participants. This work proved single channel was suitable to classify four separate finger flexions. Flexor digitorum superficial is muscle was used to extract four different finger gestures. Wavelet maximum was used to decompose sEMG and Twin Support Vector Machines (TSVM) was used to identify four finger flexions. Identification algorithm was verified on one trans-radial amputated and 11 able-bodied subject. Identification result of four finger gestures from single channel sEMG showed that accuracy and sensitivity of 81% and 84% for one trans-radial amputated and 93% and 94% for able-bodied was achieved respectively. In[12] the author proposed identification of hand gestures using RBFNN where two sEMG signals were collected from forearm to classify five hand motions such as grip, open hand, wrist flexion, wrist extension and rest position using Radial Basis Function Neural Network (RBFNN). Experimental findings demonstrated that the highest average classification accuracy was 93% achieved using RBF based on Root Mean Square (RMS), Auto Regressive model (AR) and energy of WAVELET coefficients (WAVELET) combination. But RBF based auto regressive model achieved 85% only.

In[13] the author explored a difference in three pattern matching algorithms for decoding finger motions using sEMG. 12 electrodes were located on the superficial flexor muscles. 4 electrodes were positioned on the superficial extensor muscles of the upper arm. 13 hand movements were classified in this study such as rest class, thumb flexion, thumb extension, index finger flexion, index finger extension, middle finger flexion, middle finger extension, ring finger flexion, ring finger extension, little finger flexion, little finger extension, thumb opposition and thumb abduction. Feature extracted by using Mean Absolute Values (MAV) and LDA (Linear Discriminate Analysis), k-nn, MLP (Multi-Layer Perceptron) were used as classifiers. Highest classification accuracy of 80.66% was achieved by LDA.

Electromyography grasp identification was proposed in[14]. Feature extraction performed using sum of wavelet decomposition coefficients and radial basis function kernel support vector machine was used as classifier. In this investigation, six subjects were participated to perform finger movements. Empirical results showed that average identification rate of 86% was achieved. Recognized electromyographic grasp along with 8-bit microcontroller was used to control five fingered robotic hands which were used 70% routine events. In[15] the author investigated multi-channel sEMG for identification of Hand gestures, six male subjects were picked for performing 11 types of hand gestures. Features were extracted by using energy ratio and concordance correlation. Cascaded-structure classifier was used to identify hand gestures. Empirical results showed that highest identification rate of 89%.

This study explores the possibility of recognizing twelve different hand gestures using neural networks.

3. Materials and Methods

3.1 Signal Acquisition

sEMG signals are extracted using AD Instrument bio-signal amplifier. The sEMG signal is acquired from flexor digitorum superficial is and extensor digitorum muscle of the healthy subject by five gold plated, cup shaped Ag-AgCl electrodes are placed the over the right forearm[16,17]. The skin is prepared with 70% of alcohol wipes and sensors are adhered using medical-grade adhesive tapes. Each electrode is detached from the other by 2 cm. Ground electrode is located in bony surface. Forearm electrode placement is shown in Figure 1.

Participants are placed in a comfortable chair wall and they are asked not to generate any extra movements during the data acquisition. Subjects are informed prior about the twelve different hand gestures tasks to be executed by changing their hand position. The following hand

gestures are performed by each subjects such as opening hand, closing hand, thumb extension, thumb flexion, index extension, index flexion, middle extension, middle flexion, ring extension, ring flexion, little extension and little flexion which are shown in Figure 2.

sEMG signals evoked through the twelve tasks which are recorded. Each recording trial lasted for 5 seconds. Ten trials are recorded for each task. Subjects are given an interval of five minutes between the each trial and data are collected in two sessions. Each session lasted five trials per each task. 120 data sets are acquired per each subject and a total of 1200 data samples from 10 subjects. Seven of the ten subjects are male while three are female. The sEMG signal is sampled at 400 Hz. Students and faculty members of Karpagam University who have participated in the experimental study voluntarily aged between 21 and 40 years. It was ensured that all participants are healthy and free from medication during the course of the study. During the signal acquisition, a notch filter is applied to eliminate the 50 Hz power line noise.

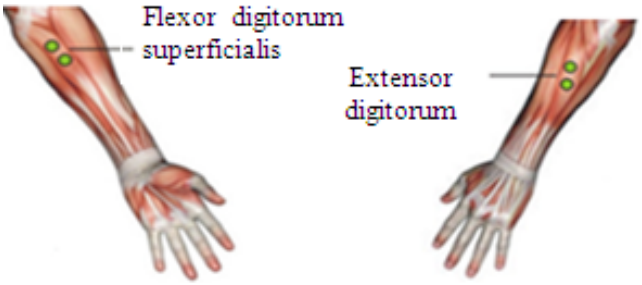

Figure 1. Sensor location for sEMG signal recording.

3.2 Spectral Analysis

The spectral of raw signals is studied using Short-Time Fourier Transform (STFT) to identify the frequency components for hand movement. STFT algorithm is applied to identify the phase content and sinusoidal frequency of a signal as it changes for different time intervals[18]. From the Figure 3, it is observed that dominant frequency range is from 0.1-150 Hz for twelve different hand movements of subject10.

3.3 Preprocessing

The raw sEMG signals are processed to extract the features. sEMG signals related to this study falls in the range of 0-500 Hz, However the predominant frequency lies in the interval of 10–150 Hz[19]. A band pass filter is used to extract the frequency. This process also removes the artifacts due to ambient noise and transducer noise.

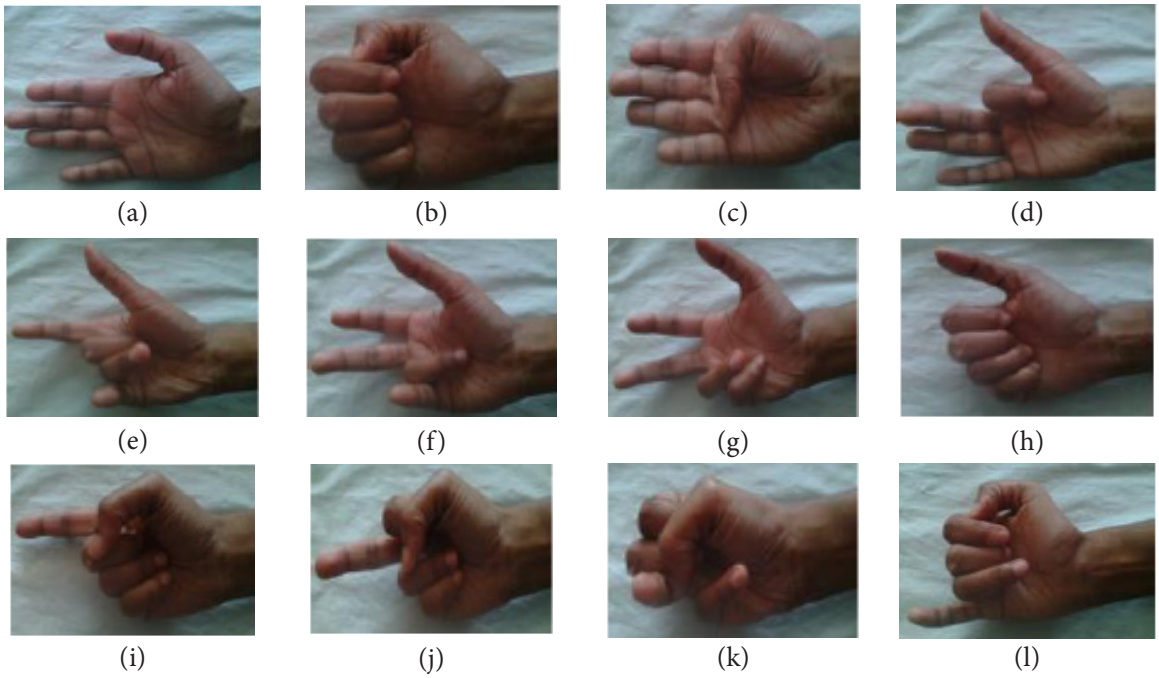

Figure 2. Twelve different finger movements **(a)** Open, **(b)** Close, **(c)** Thumb flexion, **(d)** Index flexion, **(e)** Middle flexion, **(f)** Ring flexion, **(g)** Little flexion, **(h)** Thumb extension, **(i)** Index extension, **(j)** Middle extension, **(k)** Ring extension, **(l)** Little extension.

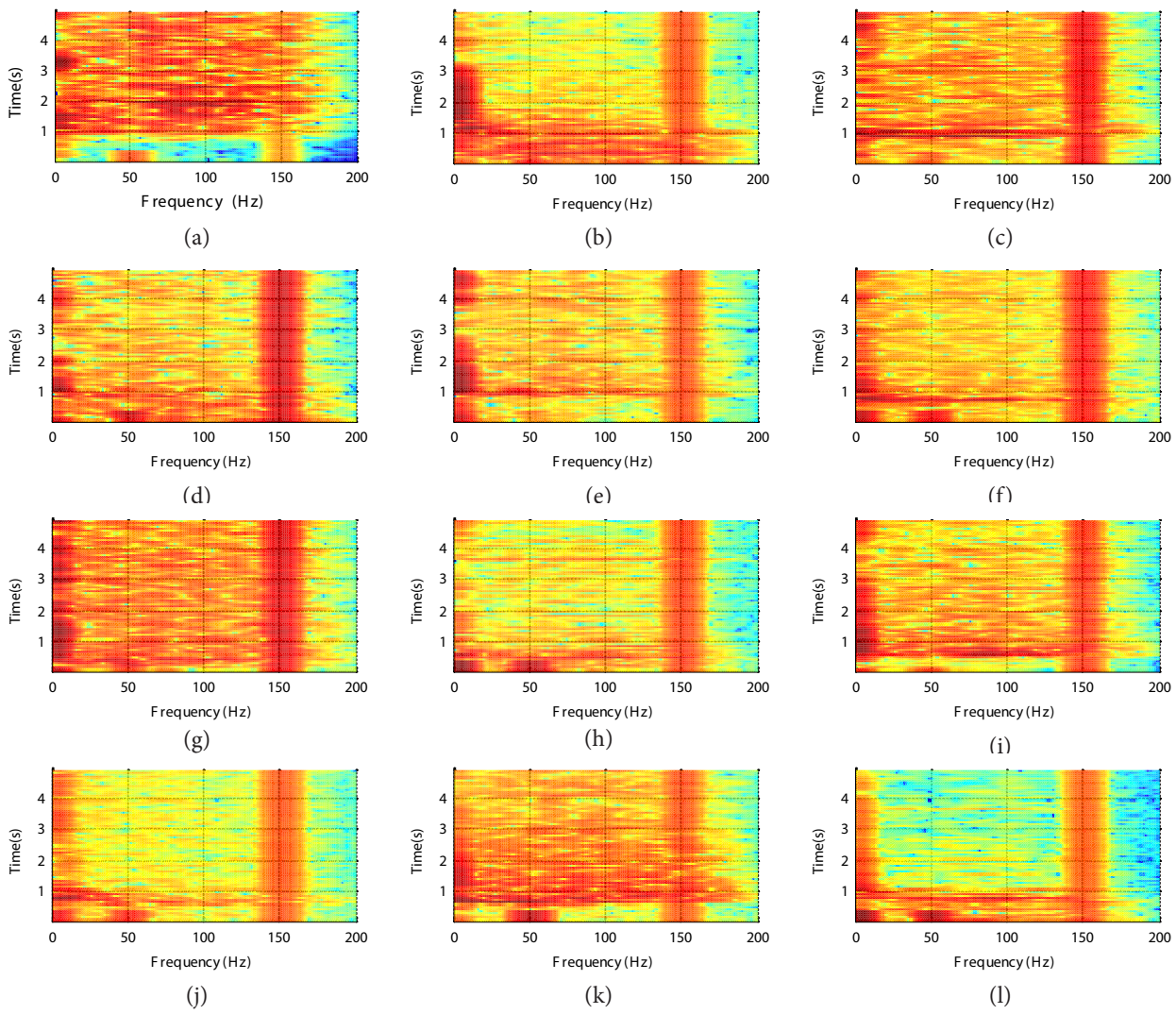

Figure 3. Spectrogram of subject 10 for twelve different finger movements **(a)** Close, **(b)** Open, **(c)** Thumb flexion, **(d)** Thumb extension, **(e)** Index flexion, **(f)** Index extension, **(g)** Middle flexion, **(h)** Middle extension, **(i)** Ring flexion, **(j)** Ring extension, **(k)** Little flexion, (**l**) Little extension.

Five frequency bands are extracted using chebyshev filter to split the signal in the range of 45 Hz. The five frequency ranges are (0.1–45) Hz, (45–90) Hz, (90–135) Hz, (135–180) Hz, (180-199) Hz. The preprocessed sEMG signals are then applied to the feature extraction stage.

3.4 Power Spectral Density Features and Their Estimation

The parametric spectrum estimation depends on the previous information of the system[20-24]. Generally used parametric method is the AR method. For the AR method, the coefficient of a signal at particular instance is derived by adding the coefficient of the past samples and summing the error estimation[25-27]. pth model order of Autoregressive (AR) process is given by

$$x[n] = -\sum_{k=1}^{p} a_k \; x[n-k] + e(n) \qquad (2)$$

Where a_k indicates AR coefficients, p indicates the model order, x(n) represents sEMG signal at the sampled point n and e(n) indicates the error term independent of previous samples. Thus, in order to obtain the estimates of AR coefficient a_k six feature extraction algorithms have been used, such as AR Burg, AR Yule Walker, AR Covariance, AR Modified Covariance, Levinson Durbin Recursion and Linear Prediction Coefficient.

3.4.1 AR Burg Method

This method uses least squares sense techniques to minimize the forward and backward prediction errors for identifying AR coefficients by fitting AR model to the sEMG signals[27]. The major benefits of the Burg estimation are high frequency resolution, stability and very efficient computation. The burg method generates the reflection coefficient automatically without the interference of autocorrelation function.

3.4.2 AR Yule-Walker Method

This method uses least squares sense techniques to minimize the forward prediction errors for identifying AR coefficients by fitting AR model to the sEMG signals. Biased estimates of the signal's autocorrelation function are also used to calculate coefficients. AR Yule Walker technique gives a stable output for all pole models. The AR coefficients are extracted by solving the normal equations[27].

$$\begin{bmatrix} q_x(0) & q^*_x(1) & q^*_x(2) & \dots & q^*_x(p) \\ q_x(1) & q_x(0) & q^*_x(1) & \dots & q^*_x(p-1) \\ q_x(2) & q_x(1) & q_x(0) & \dots & q^*_x(p-2) \\ \vdots & & & & \\ q_x(p) & q_x(p-1) & q_x(p-2) & \dots & q_x(0) \end{bmatrix} \begin{bmatrix} 1 \\ a_p(1) \\ a_p(2) \\ \vdots \\ a_p(p) \end{bmatrix} = -b(0) \begin{bmatrix} 1 \\ 0 \\ 0 \\ \vdots \\ 0 \end{bmatrix} \quad (3)$$

Once the AR parameters have been estimated, then the AR spectral estimate is computed as

$$\hat{p}_{AR}(e^{jw}) = \frac{b(0)}{1+\sum_{k=1}^{p} a_p(k) e^{-jkw}} \quad (4)$$

Where,

$$qx(k) = \frac{1}{N}\sum_{n=0}^{N-1-k} x(n+k)x*(n);\ k = 0,1,\dots,p \quad (5)$$

$$b(0) = qx(0) + \sum_{k=1}^{p} a_p(k) q_x(k) \quad (6)$$

3.4.3 AR Covariance Method

This method uses least squares sense techniques to minimize the forward prediction errors for identifying AR coefficients by fitting AR model to the sEMG signals. When comparing the Yule-Walker AR estimation, Covariance AR estimation produces higher resolution spectrum for short data records. The linear equations are solved in order to obtain the results of the covariance techniques [27],

$$\begin{bmatrix} q_x(1,1) & q_x(2,1) & \dots & q_x(p,1) \\ q_x(1,2) & q_x(2,2) & \dots & q_x(p,2) \\ & \vdots & & \\ q_x(1,p) & q_x(2,p) & q_x(p,p) & \end{bmatrix} \begin{bmatrix} a_p(1) \\ a_p(2) \\ \vdots \\ a_p(p) \end{bmatrix} = - \begin{bmatrix} q_x(0,1) \\ q_x(0,2) \\ \vdots \\ q_x(0,p) \end{bmatrix} \quad (7)$$

Where,

$$qx(k,l) = \frac{1}{N}\sum_{n=p}^{N-1} x(n-l)x*(n-k);\ k = 0,1,\dots,p \quad (8)$$

In this method, for calculating autocorrelation matrix windowing is not necessary.

3.4.4 AR Modified Covariance Method

This method uses least squares sense techniques to minimize the forward and backward prediction errors for identifying AR coefficients by fitting AR model to the sEMG signals[27]. The linear equations are solved along with equation (7) in order to obtain the results of the modified covariance techniques.

$$qx(k,l) = \frac{1}{N}\sum_{n=p}^{N-1}[fx(n-l)x*(n-k) + (n-p+l)x*(n-p+k)] \quad (9)$$

3.4.5 Levinson-Durbin Recursive Algorithm

An alternative technique of evaluating the AR coefficients is provided by Levinson-Durbin recursive algorithm. The method utilizes the important property that the coefficient of AR (k) process can be evaluated from the parameters of AR (k-1) plus k value of the auto correlation function. First order AR coefficient of the signal is first obtained thus, the algorithm proceeds recursively up to the order p.

$$\hat{R} = \begin{bmatrix} \hat{q}(0) & \hat{q}(-1) & \dots & \hat{q}(-p+1) \\ \hat{q}(1) & \hat{q}(0) & \dots & \hat{q}(-p+2) \\ & \vdots & & \\ \hat{q}(p-1) & \dots & \hat{q}(1) & \hat{q}(0) \end{bmatrix} \quad (10)$$

Where $\hat{R}$ is the p*p matrix

$$\hat{q} = [\hat{q}[1], \hat{q}[2], \dots \hat{q}[p]]^T \quad (11)$$

$$a = \begin{bmatrix} 1 \\ a(1) \\ \vdots \\ a(p) \end{bmatrix} \quad (12)$$

Where , $\hat{R}$ is auto correlation matrix
a is prediction co efficient
p is prediction order
$\hat{q}$ is vector
The parameters are estimated by

$$\hat{a} = -\hat{R}\hat{q} \quad (13)$$

3.4.6 *Linear Prediction Coefficient Analysis (LPC)*

In sEMG modeled LPC, every coefficient is evaluated as linear weighted sum of the previous p coefficient, where p indicates prediction order. When x (n) is the current coefficient, then it is foreseen by the previous p coefficients as

$$\hat{x}(n) = -\sum_{k=1}^{p} a_k\, x(n-k) \quad (14)$$

Levinson-Durbin recursive algorithm is used to calculate a liner prediction coefficient which is known as LPC analysis[28,29]. In all the six feature extraction techniques model order is fixed as 4 for better accuracy based on trial and error process and ten features are extracted for each task per trial. A total dataset consisting of 120 data samples for each subject is obtained to train and test the neural network. Figure 4 shows PSD plot using AR Burg, from the plot it is observed that every movement is taken into this experiment has unique pattern.

3.5 SignalClassification

Artificial Neural Network (ANN) is mainly used to identify the muscle activation from sEMG signal. While using ANN, the number of variables are minimized and abstained from establishing a complex mathematical model[30-32]. In this study, General Regression Neural Network, Probabilistic Neural Network and Radial Basis Function Neural Network are used to classify the sEMG data signals.

One of the special cases of multilayer neural networks is RBFNN which has four nodes such as input node, hidden node, pattern node and output node[33-35]. Hidden nodes perform radius distance between training and testing vector which is called radial basis function. Gaussian function is one of the important radial basis functions. The output node uses the least squares techniques for continuous learning.

PNN is predominantly a classifier which creates probability density functions in pattern layer by applying supervised training. It has four nodes such as input node, hidden node, pattern node and output node. PNN uses competitive learning based on multivariate probability estimation[36,37] GRNN and PNN have same architectures, but the fundamentals are different[38-40]. The target variable of the GRNN is continuous which performs regression while the target variable of the PNN is categorically performing classification.

For training and testing the neural networks 75% and 100% of data are used consequentially. The input, output and hidden neurons are namely 10, 10 and 4 respectively to identify the hand movements. The testing error factor is set as 0.1 and the training error factor is set as 0.001.

4. Result and Discussion

4.1 Network based Classification

The performance of the RBFNN is shown in Figure 5, for the six parametric feature sets. It is observed that AR Burg outdid the other feature sets with the highest mean accuracy of 94.04% for subject 10 and the lowest mean accuracy of 89.92% for subject 7. The next best performance is observed for the AR Yule feature sets at 92.38% for subject 10 and the lowest mean accuracy for the same feature sets is 89.58% for subject 7. Figure 6, depicts the classification accuracy of PNN for the six parametric features, it is evident from the result that AR Burg again outperformed other feature sets with the highest mean accuracy of 92.16% for subject 10 and the lowest mean accuracy of 89.21% for subject 7.

The classification accuracy of GRNN with six parametric features are shown in Figure 7, again it is observed that the maximum classification accuracy is with the AR Burg feature sets at 92.04% for subject 10 and the lowest mean accuracy of 88.75% for subject 7. In network based classification, RBFNN is well identified pattern this is because of the advantages of easy design, good generalization ability and good tolerance to input noise.

4.2 Subject based Classification

From the 180 developed network models, it is seen that the data from subject 10 is obtained highest accuracy levels in the range of 90.37% to 94.04% as shown in Figure 8. The least performance accuracy is observed for subject 7 with a range of 88.04% to 89.92% as shown in Figure 9. Subject 10 participated in the experiments for a long period when comparing to other subjects. The muscular flexion is also better in the subject at fitness training on daily basis. While subject 7 has a lanky physique. The other eight subjects

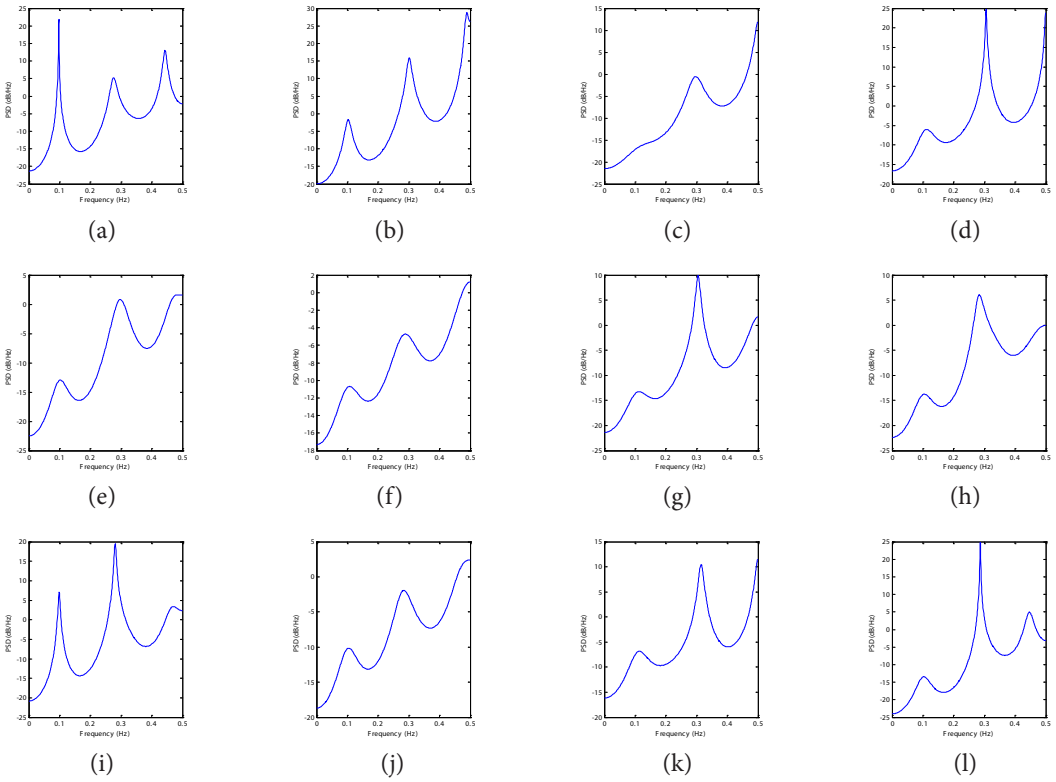

Figure 4. PSD plot for 12 different hand movements of subject 10 using AR Burg method. **(a)**close **(b)** open **(c)** thumb extension **(d)** thumb flexion **(e)** index extension **(f)** index flexion **(g)** middle extension **(h)** middle flexion **(i)** ring extension **(j)** ring flexion **(k)** little extension **(l)** little flexion

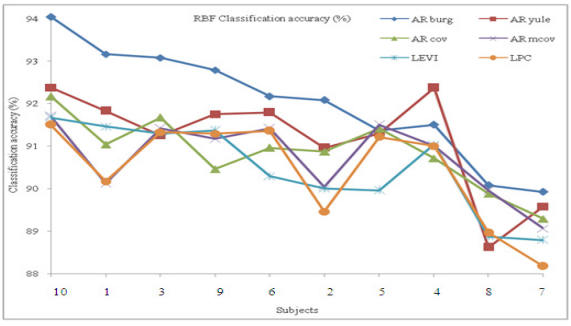

Figure 5. Classification results of RBFNN using six parametric features

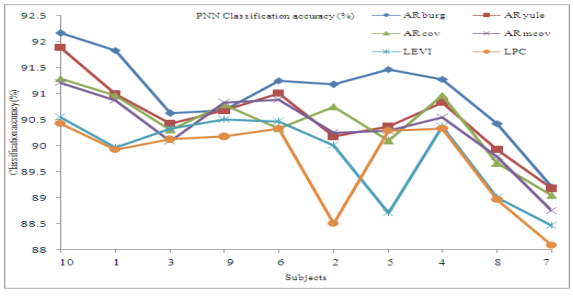

Figure 6. Classification results of PNN using six parametric features.

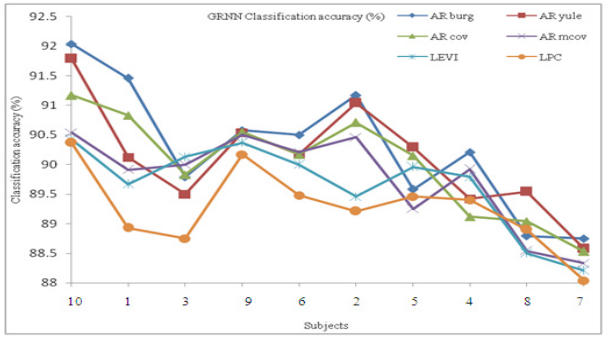

Figure 7. Classification results of GRNN using six parametric features.

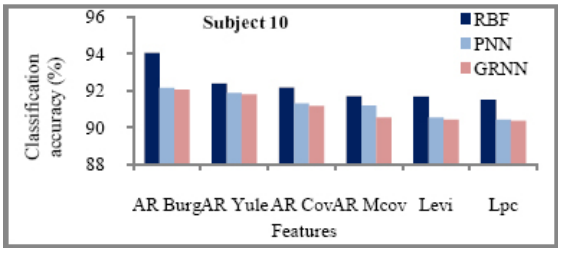

Figure 8. Classification results of subject10 for three neural networks using six parametric features.

are healthy who have not any regular fitness exercises. The next best performances are seen in female subjects who are discussed in detail in the next section.

4.3 Gender based Classification

The gender based classification results for three neural networks are shown in Figure 10, 11 and 12. It is observed from the results that the females performed better than males in all the cases without performing any regular fitness training. Mean accuracy range for the female subjects with RBFNN varies from 90.21% to 92.25% and mean accuracy range for the male subjects with RBFNN varies from 90.54% to 91.92%.

In gender based classification, females found easier to control the system than males because females are significantly more fatigue resistance than males and also they are capable to sustain their task longer than males[41].

4.4 Age Group based Classification

An analysis is also attempted to see the variations in the performance of the algorithms based on the age group of the subjects. The ten subject data are split into three categories namely 21-25 years, 26-30 years and 31-40 years. The performance results are shown in Figure 13 to 15.

It is observed from the results that sEMG data is collected from the subjects in the age group of 25-30 years

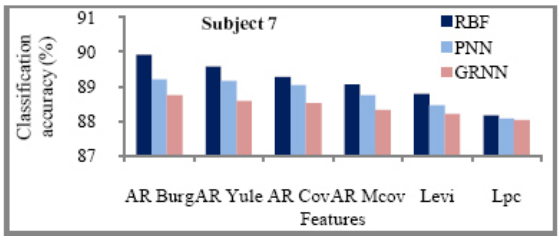

Figure 9. Classification results of subject7 for three neural networks using six parametric features.

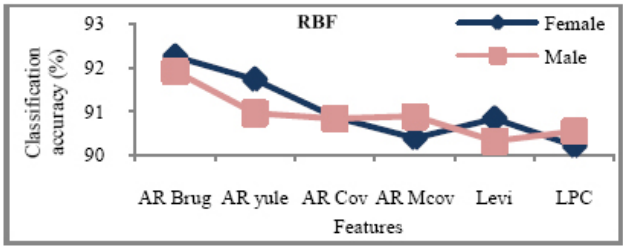

Figure 10. Gender based Classification for RBFNN using six parametric features.

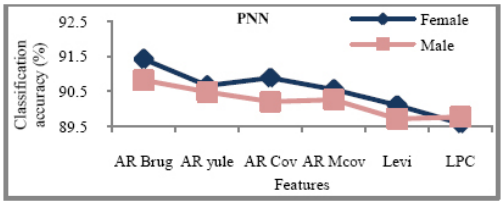

Figure 11. Gender based Classification for PNN using six parametric features.

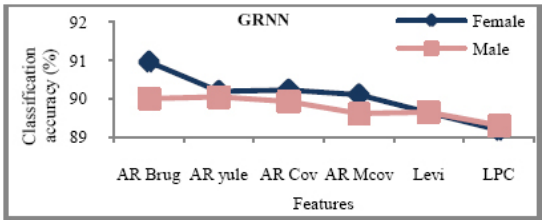

Figure 12. Gender based Classification for GRNN using six parametric features.

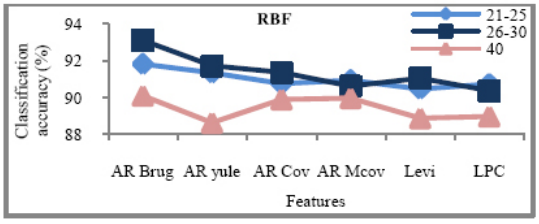

Figure 13. Age group based Classification for RBFNN using six parametric features.

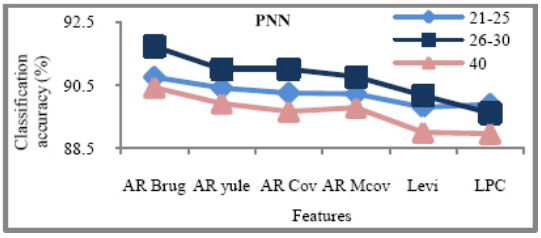

Figure 14. Age group based Classification for PNN using six parametric features.

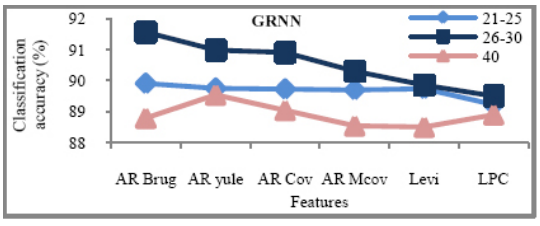

Figure 15. Age group based Classification for GRNN using six parametric features.

has better performance accuracies when comparing to the other age groups which is seen in all the three networks used. Highest performance accuracies are again observed for the AR Burg feature sets for all the networks.

5. Conclusion

In this paper, the feasibility of recognizing twelve hand gestures from the sEMG of the hand and finger movements, neural networks were investigated. Six feature autoregressive algorithms and three neural networks were used to design a suitable algorithm for recognizing the twelve hand gestures. sEMG data from ten subjects were collected which was used in the experiments. It was observed from the empirical results that the AR Burg and RBFNN combination had the highest recognition accuracy rate of 94.04%. Investigations also proved that recognition accuracy of sEMG signals were better for females when comparing to males. It was also observed from the results that the subjects at the age of 26-30 years had better muscle flexion when comparing to the other age groups in this study. However, the study is required to verify the performance of the proposed algorithms in the online recognition of sEMG signals which can be applied in HMI.

6. Reference

1. Aishwarya R, Prabhu M, Sumatran G, Anusiya M. Feature extraction for EMG based prostheses control. ICTACT Journal on Soft Computing. 2013; 3(2):472–7.
2. Zecca M, Micera S, Carrozza M, Dario P. Control of multifunctional prosthetic hands by processing the electromyographic signal. Biomedical engineering. 2002; 30(4–6):459–85.
3. Neogi B, Mukherjee S, Das A, Ghosal S, Tibarewala T. Design and implementation of prosthetic arm using gear motor control technique with appropriate testing. International Journal of Computer Applications in Engineering Technology and Sciences. 2011; 3(1):281–5.
4. Saravanan N, Kazi MS. Biosignal based human machine interface for robotic arm. 2012.
5. Panagiotis K, Artemiadis, Kostas J. Kiriakopoulos. EMG-based control of a robot arm using low-dimensional embeddings. IEEE Transactions on Robotics. 2010; 26(2):393–8.
6. Ren J, Liu TJ, Huang Y, Yao D. A study of Electromyogram based on human-computer interface. Journal of Electronic Science and Technology of China. 2009; 7(1):69–73.
7. Ahsan R, IbrahimyI, KhalifaO. EMG signal classification for human computer interaction: A review. European Journal of Scientific Research. 2009; 33(3):480–501.
8. Choi C, Kim J. A real-time EMG-based assistive computer interface for the upper limb disabled. IEEE Proceedings, 10th International Conference on Rehabilitation Robotics; Noordwijk. 2007. p. 459–62.
9. Dalal A. Design of wireless EMG and its use in the classification of finger movements [Thesis, fall]. 2012.
10. Rubana H, Chowdhury C, Mamun BI, Reaz R. Mohd Alauddin Bin Mohd Ali, Bakar, Kalaivani Chellappan C. Surface electromyography signal processing and classification techniques. Sensors. 2013; 13(9):12431–66.
11. Kumar DK, Arjunan SP, Singh VP. Towards identification of finger flexions using single channel surface electromyography – able bodied and amputee subjects. Journal of Neuro Engineering and Rehabilitation. 2013; 10(50):2–7.
12. Omari FA, Liu G, Ding Y. Classification of hand motions using RBF neural network based on extracted surface electromyography signal. Sensors and Transducers. 2014; 167(3):19–22.
13. Antfolk C, Sebelius F. A comparison between three pattern recognition algorithms for decoding finger movements using surface EMG. MEC Raising the Standard Proceedings of the Myoelectric Controls/Powered Prosthetics Symposium Fredericton; 2011. p. 14–9.
14. Nayan M, Kakoty K, Kaibarta M, Shyamanta M, Hazarika H. Electromyographic grasp recognition for a five fingered robotic hand. International Journal of Robotics and Automation. 2013; l2(1):1–10.
15. Tang X, Liu X, Congyi Lv, Sun D. Hand motion classification using a multi-channel surface electromyography sensor. Sensors. 2012; 12(2):1130–47.
16. Fougner AL. Proportional my electric control of multifunction upper-limb prosthesis [thesis]. Canada: University of New Brunswick; 2007. p. 1–64.
17. Phinyomark A, Phukpattaranont P, Limsakul C. Application of linear discriminate analysis in dimensionality reduction for hand motion classification. Measurement Science Review. 2012; 12(3):82–9.
18. Hema CR, Paulraj MP, Ramkumar S. Classification of eye movements using electrooculography and neural networks. International Journal of Human Computer Interaction. 2014; 5(4):51–63.
19. Phinyomark A, Limsaku C. EMG feature extraction for tolerance of 50 HZ interference. International Conference on Engineering Technologies. 2009; p. 289–93.
20. Herle S, Man S, Lazea G, Raica P. Myoelectric control strategies for a human upper limb prosthesis. Control Engineering and Applied Informatics. 2012; 14(1):58–66.
21. Aishwarya R, Prabhu M, Sumithra G, Anusiya M. Feature extraction for EMG based prostheses control. ICTACT Journal on Soft Computing. 2013; 3(2):472–7.

22. Park SH, Lee SP. EMG pattern recognition based on artificial intelligence techniques. IEEE Transactions on Rehabilitation Engineering. 1998; 6(4):400–5.
23. Hema CR, Elakkiya A, Paulraj MP. Biometric identification using electroencephalography. International Journal of Computer Applications. 2014; 105(8):17–22.
24. Shradhanjali A, Chowdhury S, Kumar N. Power spectral density estimation of EMG signals using parametric and non-parametric approach. Global Advanced Research Journal of Engineering, Technology and Innovation. 2013; 2(4):111–7.
25. Choi HL, Byun HJ, Song WJ, Son JW, Lim JT. On pattern classification of EMG signals for walking motions. Artificial Life and Robotics. 2000; 4(4):193–7.
26. Ahmet S, Yilmaz Y Alkan A, Musa H, Asyali A. Applications of parametric spectral estimation methods on detection of power system harmonics. Electric Power Systems Research. 2008; 78(4): 683–93.
27. Abraham B, Lal MJ, Thomas A. High resolution spectral analysis useful for the development of radar altimeter. International Journal of Innovative Research in Electrical, Electronics, Instrumentation and Control Engineering. 2013; 1(9):407–12.
28. Pazhanirajan P, Dhanalakshmi D. EEG Signal classification using linear predictive cepstrum coefficient features. International Journal of Computer Applications. 2013; 73(1):28–31.
29. Khoshnoud S, Ebrahimnezhad H. Classification of Arrhythmias using Linear Predictive Coefficients and Probabilistic Neural Network. Applied Medical Informatics. 2013; 33(3):55–62.
30. Hema CR, Ramkumar S, Paulraj MP. Identifying eye movements using neural networks for human computer interaction. International Journal of Computer Applications. 2014; 105(8):18–26.
31. Ramalingam VV, Mohan S, Sugumaran V. Prosthetic arm control using Clonal Selection Classification Algorithm (CSCA) - A statistical learning approach. Indian Journal of Science and Technology. 2016; 9(16):1–8.
32. Khoobjo E. New hybrid approach to control the arm of flexible robots by using neural networks, fuzzy algorithms and particle swarm optimization algorithm. Indian Journal of Science and Technology. 2015; 8(35):1–5.
33. Hema CR, Paulraj MP, Nagarajan N, Yaacob S. Segmentation and location computation of bin objects. International Journal of Advanced Robotic Systems. 2007; 4(1):57–62.
34. Sood M, Kumar V, Bhooshan B. Comparison of machine learning methods for prediction of epilepsy by neurophysiologic EEG. International Journal of Pharma and Bio Sciences. 2014; 5(12):6–15.
35. Manjunatha R, Badari NP, Hema Chandra Reddy K, Vijaya Kumar Reddy K. Radial basis function neural networks in prediction and modeling of diesel engine emissions operated for biodiesel blends under varying operating conditions. Indian Journal of Science and Technology. 2012; 5(3):2307–12.
36. Yu H, Xie T, Paszczynski S, Wilamowski BM. Advantages of radial basis function networks for dynamic system design. IEEE Transactions on Industrial Electronics. 2011; 58(12):5438–50.
37. Shreepad S, Sawant S, Preeti S, Topannavar T. Introduction to probabilistic neural network-used for image classifications. International Journal of Advanced Research in Computer Science and Software Engineering. 2015; 5(4):279–83.
38. Hannan SA, Manza RR, Ramteke RJ. Generalized regression neural network and radial basis function for heart disease diagnosis. International Journal of Computer Applications. 2010; 7(13):7–13.
39. Shang X. The recognition and research of improved probabilistic neural network. Second International Conference on Computer and Information Application. 2012; p. 1294–7.
40. Ghaderzadeh M, Fein R, Standring A. Comparing performance of different neural networks for early detection of cancer from benign hyperplasia of prostat. Applied Medical Informatics. 2013; 33(3):45–54.
41. Keith G, Avin A, Webber W, Maureen R, Naughton N, Brett W, Ford F, Amy M, Stark S, Haley E, Moore A, Gentile J, Laura A, Law F, Maya N, Monitto M. Sex differences in fatigue resistance are muscle group dependent. Medicine and Science in Sports and Exercise. 2010; 42(10):1943–50.